ADVANCES IN DOPPLER SONAR TECHNOLOGY

Robert Pinkel, Mark Merrifield, Jerome Smith and Hans Ramm

Marine Physical Laboratory
Scripps Institution of Oceanography
University of California, San Diego
9500 Gilman Drive
La Jolla, CA 92093-0213

Abstract - There has been significant recent progress in the development of Doppler sonar systems for marine research. Major advances include the development of side-scan Doppler systems for surface wave, ship wake and Langmuir cell research, the development of coded pulses for improved sonar precision, and the development of phased array Doppler sonar for 3-D (x,y,t) imaging of flow fields. Major challenges remain to understand the detailed behavior of the physical and biological scatterers on which these systems rely. Further effort is required to develop instruments which are robust with respect to clutter from river bottoms, ice keels, etc. As these issues are resolved, the role of acoustic remote sensing in both environment monitoring and scientific research should expand.

I) Introduction

In the five years since the preceding Conference on Current Measurement, there has been significant progress in the development of acoustic backscatter sensing systems for ocean research. Here we focus on systems recently developed at the Marine Physical Laboratory of Scripps Institution of Oceanography. Specific examples of pulse-to-pulse coherent Doppler sonars (II), coded pulse sonars (III), surface scanning sonars (IV), and multi-beam imaging sonars (V), are presented.

II) Coherent Sonar Observations in the Arctic

In the upper ocean, the classical logarithmic constant stress layer is of order 10 m in depth, roughly ten percent of the typical mixed-layer depth. In the open sea, boundary layer flows are significantly affected by surface waves and Langmuir cells. Large scale lateral pressure gradients from internal wave and mesoscale flows cause convergence and divergence of the layer. Many of these complexities can be avoided or minimized by working under the ice in the Arctic. Here surface-wave-related effects are absent. Internal wave energy levels are low relative to typical open ocean values. Ice motion (lateral stress gradients in the ice), as well as pressure gradients in the water, can drive boundary layer flows. However, since ice-water velocity differences rarely exceed 20 cm s^{-1}, shear levels in the Arctic boundary layer are low, requiring sensitive measurement systems for their detection.

In the 1989 Coordinated Eastern Arctic Experiment CEAREX, a hybrid coherent - broadband incoherent Doppler sonar was constructed for internal wave and boundary layer research (Fig. 1). In the coherent mode, a sequence of eight pulses was transmitted at a .04 s pulse repetition rate (prr), followed by a second set of eight at a .05 s prr. These coherent bursts occurred at 1.5 s intervals, with a long range coded incoherent transmission occuring between bursts. A special set of transmit transducers, separated vertically and canted relative to the receivers, was used for the coherent transmissions. The overlap region, defined by the intersection of the transmit and receive beam patterns, extends from 6 to 40 m. The limited range of this overlap minimizes "range aliasing", the contamination of the echo from the most recent transmission by more distant returns from previous transmissions.

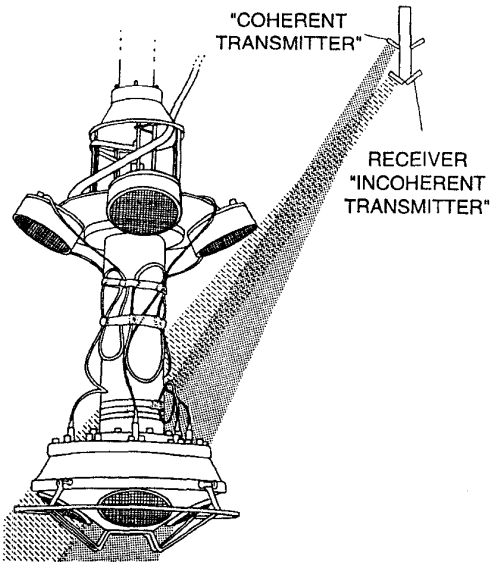

Fig. 1 The 161 kHz CEAREX sonar. Short pulse trains were transmitted from the upper transducers for subsequent coherent processing. Longer, incoherent codes were transmitted from the lower transducers. All signals were received on the lower transducers.

Individual transmissions consisted of 4- bit Barker codes with .2 ms per bit. This corresponds to 1 m range resolution, .86 m depth resolution at the 30 degree slant angle of the beams. Averages of echo intensity I(r) and pulse-to-pulse covariance $R(r,T_i)$ were formed every .5 m in range and 30 s in time. Data were recorded continuously during 4-29 April, 1989.

Each coherent prr corresponds to a specific set of alias velocities. $\Delta V_{alias} = 5.8 cm s^{-1}, 4.6 cm s^{-1}$ for the T_1 =.04 and T_2 =.05 s prr's respectively. Initially, the algorithm

$$\hat{V} = \frac{\lambda}{4\pi(T_2 - T_1)} \arg\left(R(T_1)R(T_2)^*\right) \qquad 1)$$

(Doviac and Zrnic (1984 eqn 7.7b)

was used to automatically select the correct alias.

While the algorithm expands the range of unambiguous velocities by (approximately) the factor $.5(T_2 + T_1)/(T_2 - T_1)$, it decreases the apparent velocity precision by this same factor. This decrease in precision is not fundamental. A variety of alternative techniques were developed to identify the correct velocity alias without degrading precision. The technique which proved most robust was to simply match the coherent velocity estimates to corresponding estimates derived from the incoherent mode sonar transmission. These had 6 m range resolution and were averaged over two minutes in time. Using

0-7803-2437-4/95/$4.00.

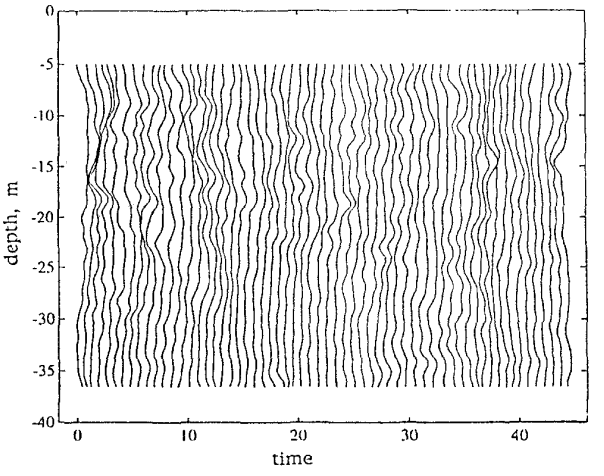

Fig. 2 A representative 20 minute record of velocity in the under ice boundary layer. Profiles, plotted at 30 s intervals, were obtained by the CEAREX sonar operating in the coherent mode. Profiles are averaged in time, resulting in a fundamental time resolution of one minute and depth resolution of .75 m. Adjacent profiles are offset by .75 cm s^{-1}, with the scale of the absicca appropriate for the left most trace.

these "low resolution" estimates as a velocity reference effectively bounds the maximum difference in reported coherent velocity to ΔV_{alias} over 6 m and 2 min. The expected geophysical shears and accelerations fall well within these bounds.

Slant velocity data from a single beam are presented in Fig. 2. Time variation in the profiles is associated with those aspects of the turbulent flow which persist through the 30 s averaging interval. There is some indication of downward propagation of events early in the record. The typical magnitude of turbulent fluctuations is less than 1 cm s^{-1}.

Using the back-to-back beams, one can estimate Reynolds stress profiles in the boundary layer. The method is based on the fact that back to back downward slanted beams measure the identical component of vertical velocity, inverted components of horizontal velocity. If θ is the angle between the sonar beam and vertical,

$$V_1 = U_1 \sin\theta + W_1 \cos\theta$$

$$V_3 = -U_3 \sin\theta + W_3 \cos\theta \qquad 2)$$

$$\langle UW \rangle = \left\langle V_1^2 - V_3^2 \right\rangle / (2 \sin\theta \cos\theta)$$

e.g.McAfee, et al., 1989) 3)

Relation 3 is valid provided the statistics of the turbulent flow are laterally homogeneous in the region between the beams.

The choice of averaging time for the stress calculation depends on both physical and statistical considerations. One can explore this issue by integrating in time the instantaneous (30 s average) values of $\left(V_1^2 - V_3^2\right)/(2 \sin\theta \cos\theta)$. Any departure in this integral from a random walk is an indication of a mean stress (e.g., Fig. 3).

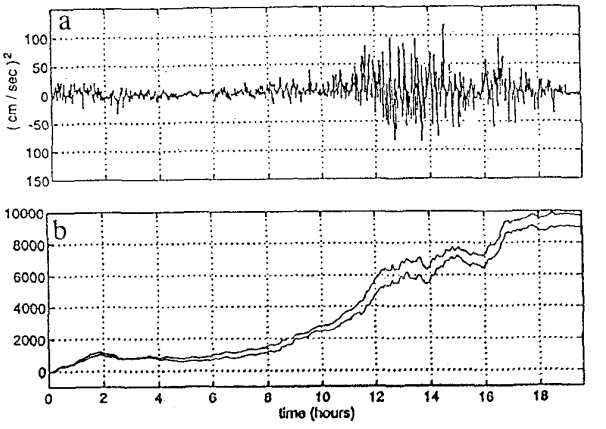

Fig. 3a The instantaneous difference in squared velocity $\left(V_1^2 - V_3^2\right)$ from the coherent sonar at 25 m range. A clear increase in turbulent activity is seen between hours 11-15 in these CEAREX under-ice measurements.

b) The time integrated difference in squared velocity at 22 m (bottom line) and 25 m (top line) range. The instantaneous slope of these lines is proportional to the Reynolds stress. The difference in slopes is proportional to the stress divergence between the two depths. Even though the sonar measurements at these two ranges are independent and the velocity fluctuations have low coherence across this distance, fine-scale details in the integrated stress are replicated.

III) Coded Pulse Incoherent Doppler Sonar

Performance bounds on incoherent Doppler systems have been estimated using methods derived for atmospheric acoustic and radar research. Theriault (1986) gives a simple approximate relation for the incoherent sounder, based on estimation of the Cramer-Rao bound:

$$\Delta V \Delta R = K c^2 f^{-1} p^{-1/2} \qquad 4)$$

where ΔV is the rms velocity imprecision. ΔR is the effective range resolution $\approx$ cT/2, where T is the duration of the transmitted pulse, c is the speed of sound, f is the acoustic frequency, and P is the number of independent incoherent averages used in forming the velocity estimate (eg, the number of transmissions). With f in Hz, the Cramer-Rao lower bound for K is $1/(8\pi)$.

Velocity precision increases with acoustic operating frequency. However, acoustic attenuation also increases with frequency. There is a tradeoff between the maximum range achievable with a given system and the expected range-velocity precision. Only by increasing the information content of the returning echo can one exceed the bounds mandated by 4).

For CEAREX, a simple "repeat-sequence" coding scheme was developed. Repeat-sequence codes are produced by taking a broad-band "subcode" and repeating it sequentially. The subcode is selected with the objective of having minimal self-correlation, except at zero lag. We consider here codes generated by reversing the sign of the signal carrier of the system at controlled intervals. The transmitted signal can be modeled as a sinusoid that is multiplied by either 1 or -1, depending on the dictates of the code. The seven-bit Barker code is shown in Fig. 4 as an example.

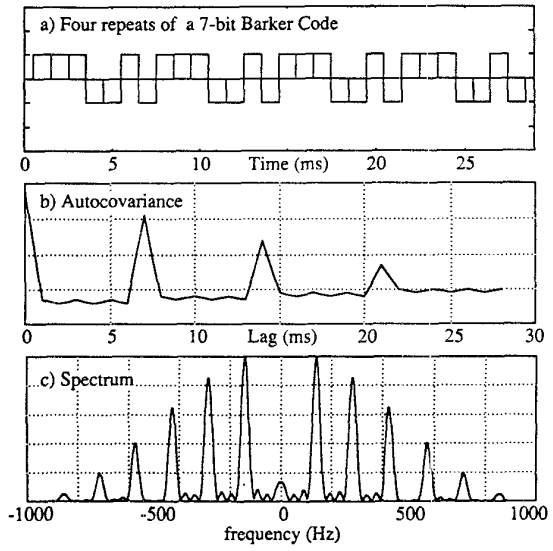

Fig. 4 (a) Schematic representation of a repeat-sequence code. The transmitted wave form consists of a 7-bit Barker code repeated four times. (b) The autocorrelation function of the repeat sequence code presented in (a). Values are small except at even multiples of the subcode length. (c) The frequency spectrum of four repeats of 7-bit Barker code. The spectrum of an uncoded sinusoidal pulse of the same duration would consist of a single peak of width equal to the width of any individual peak in the above spectrum.

The performance of a repeat sequence code is given by:

$$\Delta V \Delta R = \frac{1}{4\pi}\left(\frac{3c^3 V_{\max}}{2Pf\Delta f}\right)^{1/2} \quad \text{(Pinkel and Smith, 1992)} \qquad 5)$$

Here it is assumed that range resolution is given by $\Delta R = (n-1)L\tau c/2$, where τ is the duration of an individual bit and L is the number of bits in the sub-code. Range averaging is performed over the corresponding interval ΔR. The maximum velocity one can resolve, without aliasing, is $V_{\max} = c/(4f\tau L)$.

Equation 5 is useful in addressing both operational and system design issues. It illustrates the capability to customize repeat sequence codes for specific "velocity variability" situations, $V_{\max}$, in addition to standard range-velocity precision constraints. This allows greater flexibility in operation than single pulse-pair codes (Edwards 1979, Brumley et al., 1990) , which represent the low $V_{\max}$ limit of the repeat sequence family.

In designing or modifying sounder systems, equation 5 indicates that net performance will vary as $(f\Delta f)^{-1/2}$ One can improve performance of an existing fixed-frequency system by increasing the bandwidth. Conversely, in considering new systems, one can double the bandwidth of a benchmark design and halve the carrier frequency, while maintaining performance. The lower-frequency sounder will have significantly greater overall range. For a fixed carrier frequency, bandwidth and range resolution, low $V_{\max}$ codes (few repeats of a long sequence) produce better velocity estimates than their higher $V_{\max}$ (many repeats of a short sequence) counterparts (eq 5). However, marine Doppler sounders are often mounted on moving ships. Maximum mean velocities of order 5 - 10 m s^{-1} can be encountered associated with the ships forward movement.

In Fig. 5 a section of zonal velocity is presented. The data are obtained from a 161 kHz sonar mounted on the R/V John Vickers. The instrument was operated continuously over a nine-month period as the ship traversed the Pacific Ocean. The section presented in Fig. 5 represents a crossing of the equatorial undercurrent, seen with the 2.5 m vertical resolution of the sonar. The 100 cm s^{-1} zonal currents are easily resolved above the measurement noise. Six repeats of a four bit code, .2 ms/bit, were used.

Subsequent to these TOGA COARE/CEPEX measurements, the sonar was removed from the ship and adapted for Arctic operation. During November 1993 the sonar was deployed through the ice in the Beaufort Sea, 74° N, 154° W, in conjunction with the SIMI ice mechanics experiment. The range of velocities expected in the Beaufort Sea is extremely small. Internal wave energy levels are typically two orders of magnitude

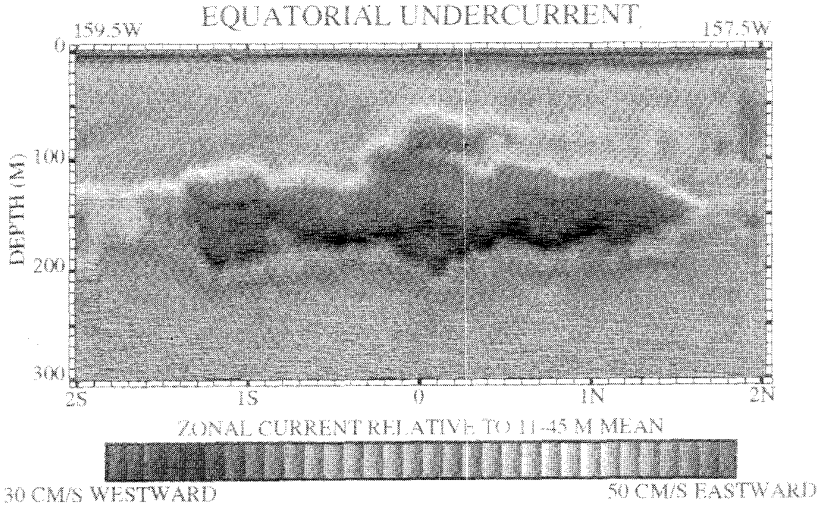

Fig. 5 A view of the Equatorial Undercurrent obtained from a 161 kHz sonar as the R/V John Vickers steamed north-eastward from 2 S, 159.5 W to 2 N, 157.5 W. The typical ships speed was 14 kts. To avoid velocity aliasing, six repeats of a 4 bit code were transmitted, .22 ms/bit. The .88 ms processing lag corresponds to a radial $V_{\max}$ of 2.65 m s^{-1}. By orienting the sonar beams at 45° angle to the direction of ships motion, and 60° down from horizontal, the ships mean velocity as well as surface swell perturbations could be accommodated.

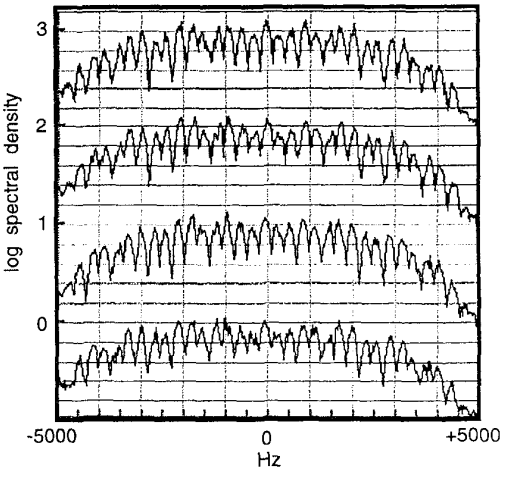

Fig. 6 The received echo spectrum corresponding to two repeats of a 17 bit code, .22 ms/bit, centered at 161 kHz. This code, with V_{max} .62 ms^{-1} is appropriate for the Beaufort Sea, where expected velocity variability is low. The four traces represent signals received simultaneously from the four beams. The frequency scale spans ±5 kHz about the carrier.

smaller than in open ocean regimes. Maximum velocities of 30 cm s^{-1} occur, associated with wind driven motion of the sea ice and the occasional passage of sub-mesoscale eddies.

In response to this low V_{max} environment, a 17 bit code was developed for the sonar. The code was repeated twice. The bit width of the code was again .2 ms. The spectrum of the recorded echo, following reflection off the extremely quiescent scatterers in the Beaufort Sea, is presented in Fig. 6. High velocity precision is required in this low energy environment. The ability to select appropriate codes for both low and high energy regimes has greatly increased the usefulness of the single instrument.

IV) Surface-Scan Doppler Sonar

In the last few years surface-scanning Doppler sonars have gained acceptance for the measurement of the sea surface velocity field. In contrast to conventional sounders, these devices transmit a fan shaped "side-scan" beam which illuminates (insonifies) a narrow stripe of the sea surface from below. The sound scatters from sub-surface micro bubbles, which provide a far stronger scattering target than the zooplankton of the ocean interior. From the Doppler shift of the echo, the velocity signatures of surface waves, Langmuir cells, sea surface fronts and internal waves can be inferred.

In Fig. 7 a four minute record from a 195 kHz surface-scanning sonar is presented. Scattering intensity (left panel) and radial velocity (right panel) are displayed. A tugboat, moving at approximately 10 kts., passes through the beam at time 13:41. The added bubbles associated with the tugboat passage produce the enhanced scattering in the V shaped region behind the tug. The bubbles are quickly collected in two regions of surface convergence in the wake, producing the patterns shown.

The right panel displays the cross-wake component of velocity. The velocity field is dominated by pre-existing surface waves which are propagating toward FLIP. Note that the leading edge of the wake is dark (velocities toward FLIP) on the left side of the tug and light on the right side. This reflects the motion of the

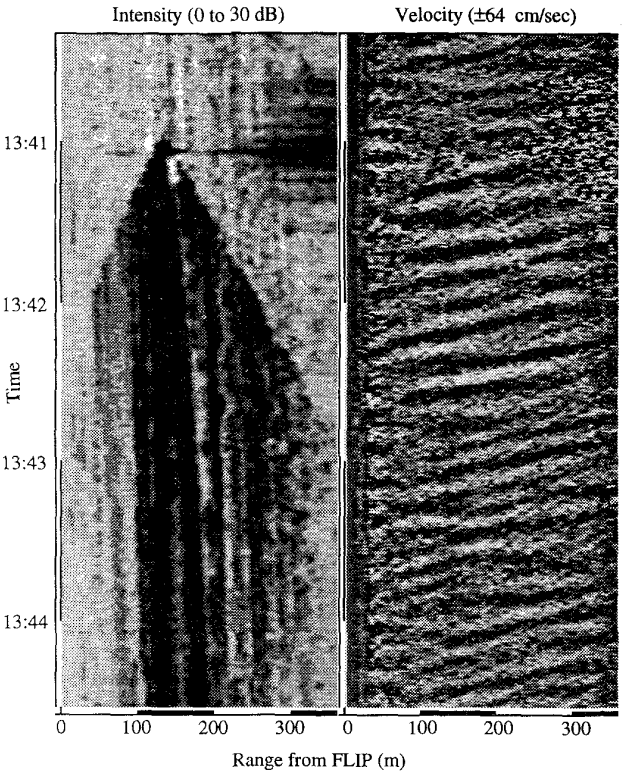

Fig. 7 Echo intensity (left) and sea surface velocity (right) from a 195 kHz surface scanning sonar mounted on the Research Platform FLIP. A tug boat passes through the beam at 13:41 PST, range 140 m, traveling normal to the beam direction. Enhanced scattering is seen from bubbles produced by the Kelvin wake (which is breaking), as well as from the bow wave of the tug. The trailing bubbles are organized into parallel streaks by a vortex pair generated with the passage of the ship. The velocity signature of the vortices can be seen beneath the signature of the ambient surface waves.

crest toward FLIP on the left, away on the right.

Less apparent are the faint light and dark streaks which are seen in the trailing wake. These time persistent features indicate a velocity divergence along the centerline of the wake with associated convergences to the outside (where the bubbles collect).

The ability of a passing ship to generate a vortex pair in the ocean surface layer suggests both engineering (full scale ship tank testing) and scientific applications. In particular, one might wish to inject a vortex pair into the oceanic mixed layer at some specific angle to the ambient Langmuir cells. The interaction of the natural and man-made vortices could be monitored in the hope of gaining further insight into the local dynamics.

V) Sector-Scan Doppler Sonar

Discreet beam acoustic sounders have been in existence for over 20 years. Each beam provides a 2-d (range-time) picture of the radial component of flow. In an attempt to extend t measurement capability to a third dimension (r,θ,t), we he constructed a phased array sector-scan Doppler sonar (Fig. 8). T

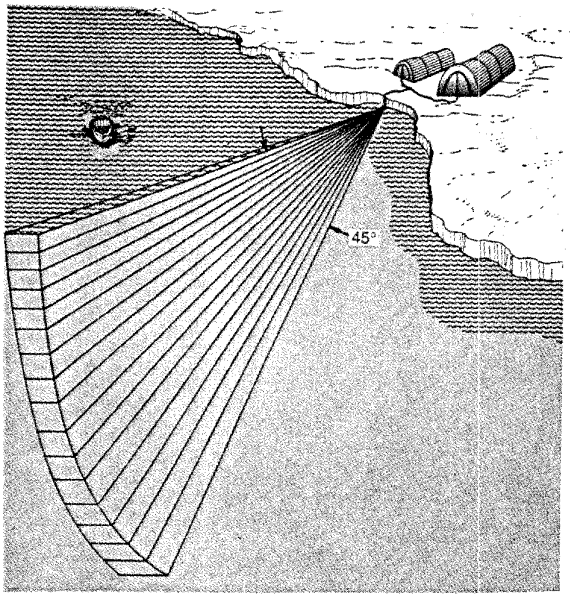

Fig. 8 Schematic diagram of the 195 kHz sector scan sonar deployed in the 1992 LEADEX experiment.

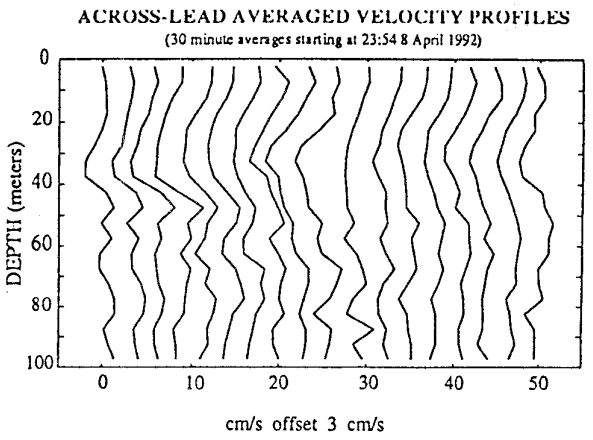

Fig. 9 A 9 hour observation of the cross lead component of velocity.

system operates at 195 kHz, transmitting a fan-shaped 45° x 2° beam from a bar transducer. The echo is received by a 16 element phased array.

The sector-scan was first deployed in April 1992, in conjunction with the Arctic Leads Experiment (LEADEX). Leads are cracks in the ice cover of the ocean. These expose freezing cold water 0°C to an atmosphere which is frequently 40°C colder. Air-sea temperature differences in the Arctic are as great as anywhere on earth. The scientific objective of the sonar deployment was to detect lead related flows such as convective cells which might be driven by local freezing processes. Quantifying the influence of ambient background flows on the near-lead environment was a parallel priority.

The technical challenge was to observe flows in the center of a lead using instruments mounted at the edge. The sector-scan design was a response to this challenge. While convective activity was apparently not present at the lead visited (LEADEX "lead 3", 6-9 April, 1992), a detailed set of vertical profiles of horizontal velocity was collected from the central section (50-250 m range average) of the lead (Fig. 9). These showed weakly sheared flow in the mixed layer (0-30 m) with stronger shears in the waters below. Heat fluxes into the lead during this time were relatively weak. The absence of obvious convective activity is thus understandable.

VI) Summary

1994 marks the twentieth year of development of Doppler sonar systems at Scripps. We now understand how to construct systems for a wide variety of scientific tasks, systems which will function in a wide variety of environmental settings. Hardware has become sufficiently robust to enable extended unattended operation. In addition to short-term scientific process studies, a longer term environmental monitoring role is emerging for these systems. River, harbor and coastal flows, as well as those in the deep sea, are now open to long term observation.

References

[1]. Brumley, B., R. Cabrera, K. Deines, and E. Terray, 1990: Performance of a broadband acoustic Doppler current profiler. Proc. of the IEEE Fourth Working Conference on Current Measurement. Institute of Electrical and Electronics Engineers, New York City, 283-289.

[2]. Doviak, R. and D. Zrnic, 1984: Doppler Radar and Weather Observations. Academic Press, Orlando, 458 pp.

[3]. Edwards, J. A., 1979: Remote measurement of water currents using correlation sonar. Presented at 98th meeting of the Acoustic Society of America, Salt Lake City, Utah.

[4]. Mc Afee, J. R., B. B. Balsley and D. S. Gage, 1989: Momentum flux measurements over mountains: problems associated with the symmetrical two beam radar technique. J. Atmospheric and Oceanic Technology. 6-3, 500-508.

[5]. Pinkel, R. and J. A. Smith, 1992: Repeat sequence coding for improved performance of Doppler sonar and sodar. J. Atmospheric and Oceanic Technology. 9-2, 149-163.

[6]. Theriault, K. B., 1986: Incoherent multibeam Doppler current profiler performance. Part I: estimate variance. J. Ocean Eng., Vol. OE-11(1), 7-15.